MULTIPLE RESONANCE VIBRATION MITIGATION ON A 54,000 HP PARALLEL SHAFT DOUBLE HELICAL SPEED INCREASER

by

B. Fred Evans

Consultant, Rotating Equipment

James F. McCraw

Project Engineer

BP Amoco

Houston, Texas

and

Greg Elliott

Project Engineer

Lufkin Industries

Lufkin, Texas

B. Fred Evans is a Consultant for Rotating Equipment within the Operations Excellence Team of BP Amoco Corporation's Upstream Technology Group, in Houston, Texas. He is responsible for providing engineering services on rotordynamics, aerodynamics, and troubleshooting dynamics related problems as well as performing design audits of proposed equipment purchases for BP Amoco's various upstream business units. Prior to joining BP Amoco, he worked for Southwest Research Institute, providing field technical services on dynamics problems for all areas of the energy industry.

Mr. Evans is a registered Professional Engineer in the State of Texas. He received BSME and MSME degrees from Texas Tech University (1974).

Jim McCraw is a Project Engineer in the Natural Gas Liquids Business Unit within BP Amoco, in Houston, Texas. He has been responsible for multiple compressor projects from initial concept to commissioned plant. Mr. McCraw is also responsible for incorporating design features on rotating equipment that improve the machine availability, reliability, and reduce maintenance costs. Prior to joining BP Amoco, he worked for Davy Powergas, Inc., and Jacobs Engineering Group on various refinery, petrochemical, and gas processing plants.

Mr. McCraw attended the University of Missouri and received his BSEE degree from Finaly Engineering College (1971).

Greg Elliott is a Project Engineer in the Power Transmission Division of Lufkin Industries, in Lufkin, Texas. He is responsible for product development including analysis, design, and engineering systems for new product lines. He also supports production engineering with finite element analyses, fatigue analyses, and other applications of engineering mechanics in machine design. Prior to joining Lufkin, he worked in research and teaching at Texas A&M University.

Mr. Elliott received B.S. and M.S. degrees (Agricultural Engineering, 1990) from Texas A&M University.

ABSTRACT

Test stand vibration measurements on a partially loaded 54,000 hp, parallel shaft, double helical speed increaser revealed synchronous resonant vibrations near normal operating speed. Further testing confirmed the lateral critical speed of the pinion was lower than originally designed due to modifications applied while the gear unit was in the test stand, which were aimed at lowering bearing pad operating temperatures under full load field conditions. The lateral critical speed was seen to increase as expected by sequentially removing the coupling spacer, adapter plate, and the hub. However, resulting vibration measurements showed a resonance remained near running speed.

Impact testing pointed to a structural, resonant axial motion of the gear case near rated operating speed. Finite element analyses of the gear unit confirmed the existence of two structural resonances with endwall *breathing* mode shapes near pinion speed. Excitation of one of these modes was provided by coupling unbalance on the rotating pinion shaft that demonstrated cross-coupling of radial forces due to unbalance and axial structural motions. The near

coincidence of the structural resonance and the lateral critical speed on the test stand provided vibration amplification above that normally expected due to either resonant condition alone. Amplification factors were moderate and significant overlap occurred between the *flanks* of the two resonances.

A two step solution was implemented to increase the resonant frequencies of both the shaft in its oil film bearings and the gear case end walls. First, a bearing clearance and preload modification were applied along with additional hot oil removal techniques. Second, a tie bar brace was added above and parallel to the pinion between the end walls of the upper section of the gear case to increase structural stiffness in an axial direction. Additional rotordynamic and finite element analyses predicted significantly improved response to unbalance. The bearing and structural modifications were installed and tested sequentially. These tests, under similar conditions as previously imposed on the unit for qualification and acceptance, were successful in proving the solution.

This paper documents measured vibrations at various stages in the investigation, results of rotordynamic and finite element analyses, bearing and gear case modifications, and final successful tests.

INTRODUCTION

An expansion project at a natural gas liquids processing facility required a compression service to return residue gas to a pipeline. The selected compression train consists of an 1800 rpm synchronous motor driving through a geared speed increaser to a centrifugal compressor. The mechanical rating at the gear mesh is 54,000 hp with a pinion speed of 5547 rpm. The gear unit was specified to meet API 613 (1995) requirements, but due to the high power rating and starting transient conditions, additional requirements were added to the purchase specification. General rating information is shown in Table 1, while Figure 1 illustrates the massive size and arrangement of the parallel shaft, double helical design. This paper deals with resolution of two resonant conditions causing increased pinion vibrations that were encountered during acceptance testing at the vendor's manufacturing facility.

Table 1. Double Helical Speed Increaser Ratings.

Rated Power	54000	horsepower
Gear Ratio	3.082:1	-
Shaft Speeds	1800 / 5547	revolutions per minute
Service Factors	2.18 / 1.6	AGMA / API
Pitch Line Velocity	27000	feet per minute

During the purchasing phase of the project, special consideration was given to the design of the gear and pinion including construction details and rotordynamic analyses. Table 2 shows the integral shaft/pinion detail information and the finished pinion is shown in Figure 2. The uploaded pinion is supported by a pair of 10 inch diameter tilting pad journal bearings with a length to diameter ratio of one. Figure 3 shows a bearing installed in the bottom half of the gear case. Close tolerances were specified for clearance and preload to control rotordynamics. To reduce bearing pad operating temperature, offset pivots were used along with oil inlet spray bar blockers (Nicholas, 1998) to increase the effectiveness of cool inlet oil as shown in Figure 4. Maximum bearing temperature rise allowed during test stand acceptance runs was 50°F while operating at 2 percent of rated power.

ROTORDYNAMIC DESIGN REVIEW

A standard rotordynamic and stability analysis was performed as per the requirements of API 613 (1995). The analysis included

Table 2. Integral Pinion Details.

Shaft Weight	3657	lb
Shaft Length	92.88	in
Bearing Span	50.64	in
Pitch Diameter	18.62	in
Speed	5547	rpm
Bearing Type	Tilt Pad	-
Load Direction	Between Pads	-
Number of Pads	4	-
Bearing Diameter	10	in
Bearing Length	10	in
Bearing Preload	0.3	-
Bearing Clearance	15	mils
Bearing Load	34000	lb

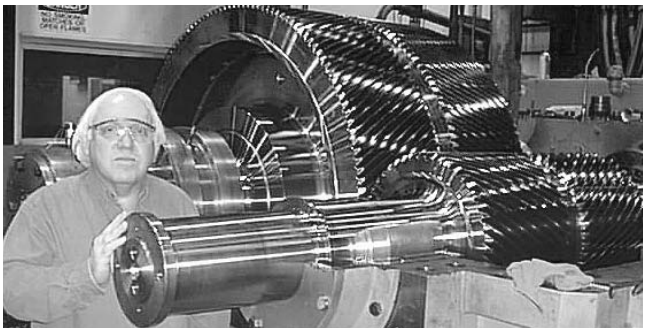

Figure 1. Pinion and Gear Installed in Gearcase.

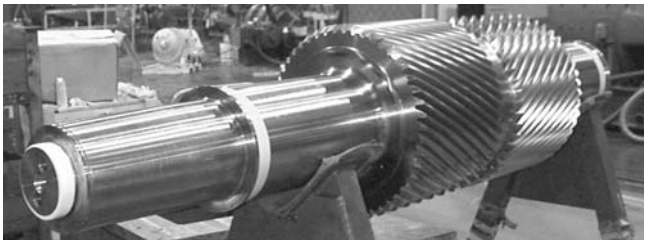

Figure 2. Pinion Viewed from Drive End.

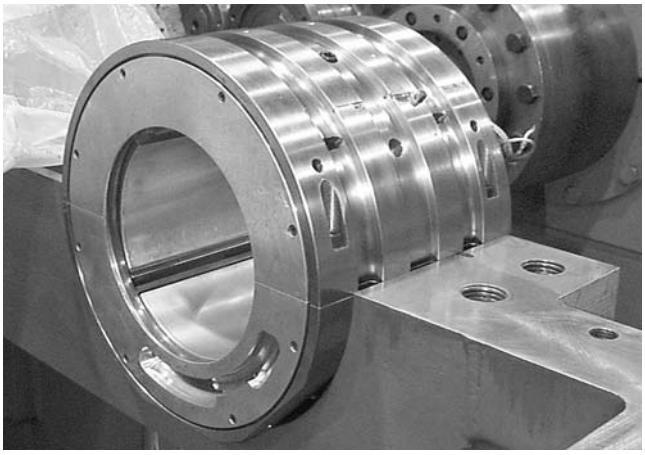

Figure 3. Pinion Bearing Viewed from Inside Gearcase.

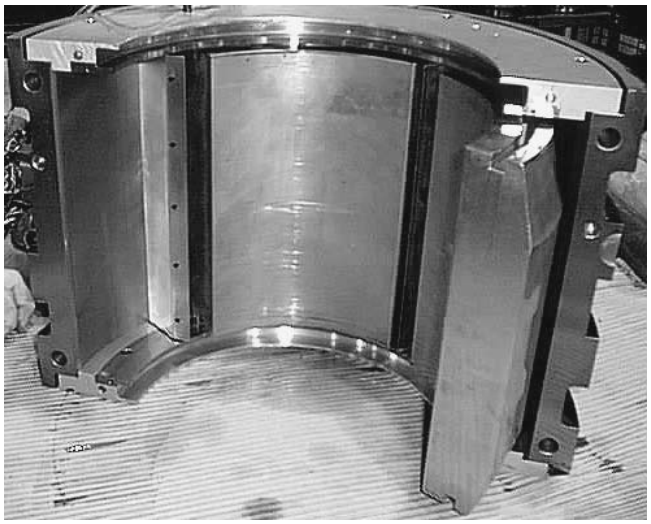

Figure 4. Pinion Bearing Split Open to Show Pads and Oil Inlet Spray Blocker Bars.

bearing design parameters to cover tolerances on preload and clearance as well as variation in applied load. The shaft was modeled, as shown in Figure 5, starting at the coupling end. The half coupling weight and inertia were modeled as added terms located at its center of gravity as determined by the coupling vendor. The undamped critical speed map is shown in Figure 6 with equivalent support stiffness curves superimposed for 100 percent load conditions in the field. These stiffness values are seen to be in the range of five to 10 million lb/in and are different for horizontal (xx) and vertical (yy) directions. This simplified analysis shows the first critical speed should be in the 7000 to 8000 rpm range, which is well beyond API 613 (1995) requirements for all critical speeds to be at least 20 percent above operating speed. Figure 7 is the undamped first critical speed mode shape at a support stiffness near expected values. It is an overhang mode of the extended (coupling) end of the shaft with a node near the blind end bearing. This mode would be very sensitive to coupling unbalance.

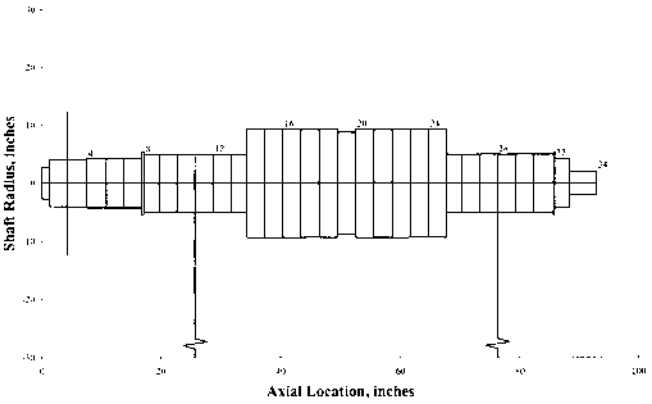

Figure 5. Rotordynamic Model of the Pinion.

Shaft support dynamic properties comprise several spring and damper analogies in series, but the oil film characteristics usually dominate other contributors. Most analyses could consider the oil film alone since it can be orders of magnitude softer than the other support springs. However, the bearings supporting the pinion in this analysis were estimated to have a stiffness of generally the same order of magnitude as the effective stiffness of all other combined parts of the support system between the bearings and

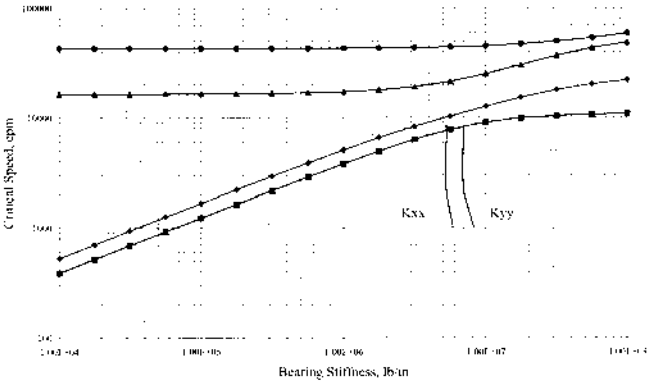

Figure 6. Pinion Undamped Critical Speed Map.

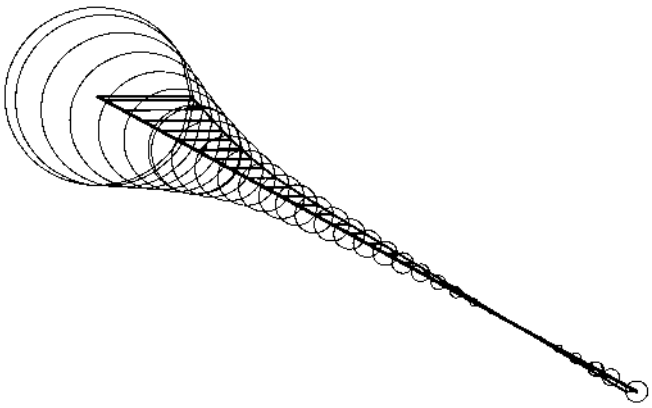

Figure 7. Pinion Undamped Mode Shape.

ground. Therefore, a range of support stiffness values was used in the analysis to cover soft and hard support for the bearings. Soft values were six and 12 million lb/in in the horizontal and vertical directions, respectively, while hard values were 10 and 20 million lb/in. This gives rise to the nonsymmetric support values even though the four pad bearings with load between the pads should have symmetric oil film stiffnesses for horizontal and vertical directions.

Calculated predictions of vibration response to coupling unbalance for the extended end bearing shaft location are shown in Figures 8 and 9 for the soft and hard support stiffness cases, respectively. The peak vibrations were predicted to be between 6980 and 7540 rpm in a horizontal direction and above 7880 rpm in the vertical direction. This illustrates the overall net decrease in predicted frequency from the undamped critical speed map referenced above due to consideration of damping and structural flexibility. In general, the results of the analysis met the design criteria and indicated no vibration or bearing pad temperature problems should exist with a nominal journal bearing assembled clearance of 1.5 mils per inch of shaft diameter. The pinion design was accepted and the gear unit built and prepared for test stand acceptance runs.

INITIAL TEST RESULTS

Initial operation of the gear unit on the manufacturer's test stand revealed higher than predicted pinion bearing temperatures as measured by resistance temperature detectors (RTDs) embedded in the bearing pads. Values measured were over 205°F in an extremely lightly loaded condition with a supply temperature of 130°F. While this was within material limits for the bearings, it was higher than expected and did not meet the specified temperature rise limit of 50°F. Additional oil flow was added to the bearings by opening the orifice diameter, but this did not lower the

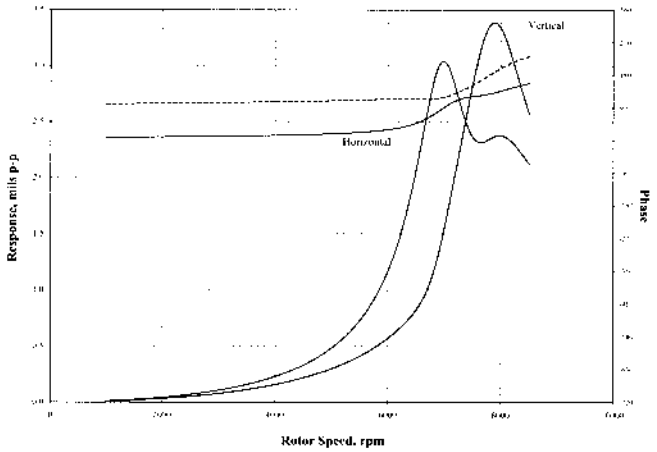

Figure 8. Response to Coupling Unbalance with Soft Supports.

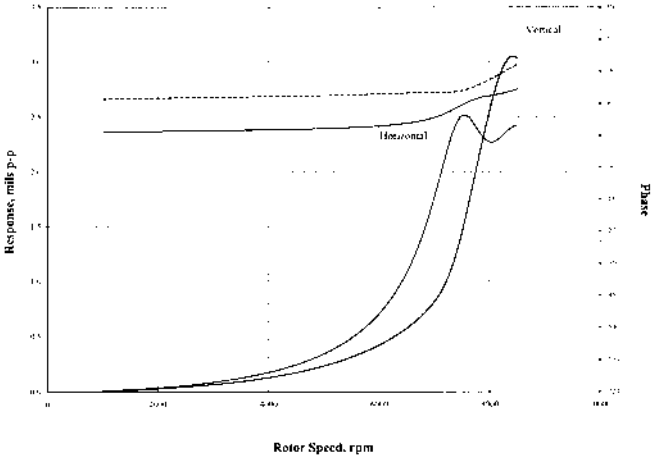

Figure 9. Response to Coupling Unbalance with Hard Supports.

temperatures. Next the bearings were modified to allow a better exit path for the hot oil in the center of the long bearing and the clearance was increased to 2.0 mils per inch of shaft diameter. The bearing end seals were also opened to a larger clearance. The clearance change was easily accommodated by changing shims in the ball and socket pivot design, and a quick review of the rotordynamic calculations was made.

The gear was run on test again and the pinion bearing pad temperatures were significantly improved to the 170 to 180°F range. Most of the improvement was attributed to more efficient removal of hot oil from the bearing housing.

Vibration measurements during a coast down run without any unbalance weight added to the coupling indicated low vibration levels within the API 613 (1995) limits. However, during overspeed tests with a coupling unbalance weight installed, a vibration peak was observed near running speed and another close to but below the required 20 percent separation margin of 6656 rpm. Figure 10 shows the vibration data recorded during the coast down from overspeed. Sufficient unbalance weight had been added to yield a peak amplitude in the 3 to 5 mil range. The data are from proximity probes installed 45 degrees either side of vertical just outboard of the extended end bearing on the pinion. The data have been processed to give a reading in true horizontal and vertical planes for easy comparison to calculated responses. In the vertical direction a peak is seen at 5600 rpm while in the horizontal direction a peak is at 6500 rpm. Data were recorded discretely every 100 rpm so the actual peaks might be at slightly different frequencies than the recorded values. The peaks appeared broad with moderate amplification factors in the range of six to nine.

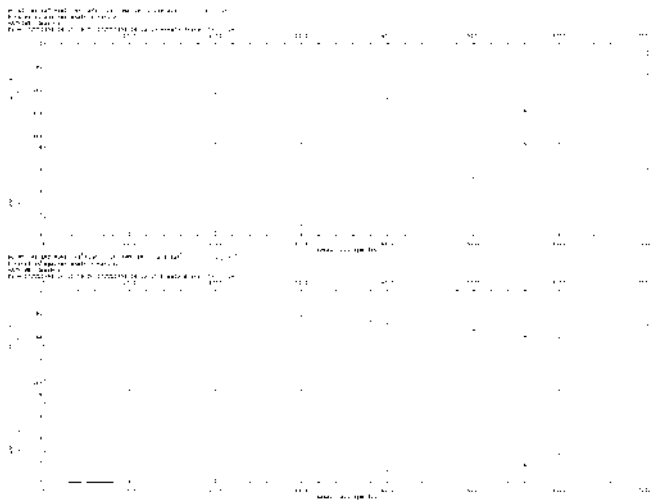

Figure 10. Pinion Extended End Measured 1× Vibration on Test Stand.

ROTORDYNAMIC REEVALUATION

An investigation was begun to determine if the bearing clearance changes from 1.5 to 2.0 mils per inch of shaft diameter had caused a critical speed to drop nearer the operating range. The combination of larger clearance and low loads on the test stand were used in the rotordynamic reevaluation. The analysis was extended to cover field conditions as well as test stand conditions with a shop coupling installed driving a slave gear and energy dissipation device.

Load force vectors imposed on the pinion journal bearings vary considerably due to transmitted power variations and the fact that the pinion is uploaded. The vertical load vector is due to the combination of forces arising from static pinion weight and transmitted forces at the mesh. The horizontal load vector is due to the separating forces generated at the mesh based upon the double helical design. Thus, both the magnitude and direction of the total load vector on the bearings are changing as either speed or power is varied. Shop conditions are vastly different from field conditions since the test stand was limited to approximately 2 percent of rated power and the field coupling was replaced by a shop coupling and adapter plate that weighed more.

For field startup conditions, the bearing load vector is a function of load torque consumed by the compressor. Various starting scenarios were considered in the early design of the compressor train, and the resulting compressor torque range as a function of speed is shown in Figure 11. The compressor torque was kept to as low a value as feasible to reduce motor starting requirements. Compressor suction pressure was controlled to be between 40 and 50 psig during the approximately 15 second startup time required by the electric motor drive. Figure 11 shows compressor load torque curves for flow conditions bounded by choke and surge for 40 and 50 psig suction pressure.

The resulting bearing load vector for startup begins as a vertically downward force due to the static weight on the bearing, and swings away from the mesh rotating approximately 150 degrees as speed and torque increase. Figure 12 shows the load vector direction for startup and operation up to full rated power. In the low power range below 15 percent of rated conditions the greatest slope is seen. The impact of this rotating load vector on bearing dynamic properties is realized when it is plotted on a schematic representation of the four tilting pad bearing shown in Figure 13. Vectors are plotted every 1000 rpm for the field startup. A vector is included for a shop test stand load of 2 percent at full speed and it is seen to be between the 1000 and 2000 rpm vectors for field startup. Also included is a vector showing the direction of th full power field condition bearing load but its magnitude would be off the scale of the graph. Bearing

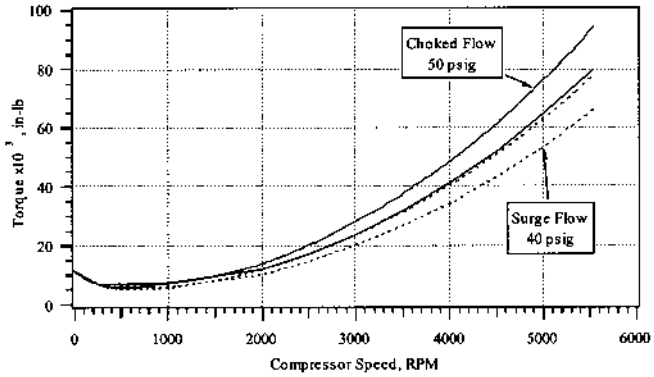

Figure 11. Gear Mesh Torque Due to Startup Load from Compressor.

static and dynamic characteristics are a function of eccentricity and attitude angle. Based on the load vector variation, the bearing operates as a load between pivot design at full load but not during startup. The dynamic characteristics can be expected to change accordingly and this was accounted for in the rotordynamic reevaluation of both shop and field conditions. This detailed an analysis is not called for by API 613 (1995).

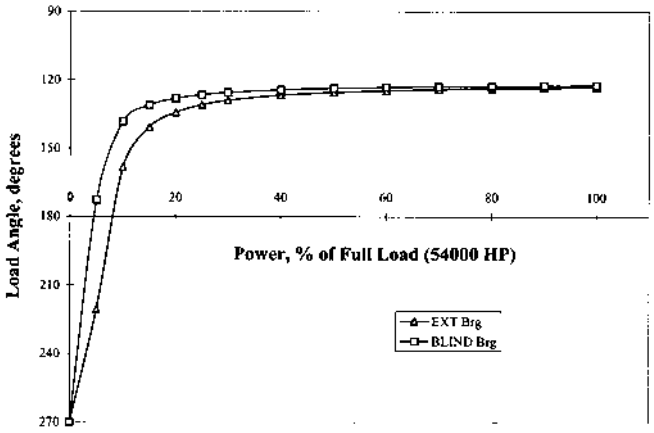

Figure 12. Pinion Bearing Load Angle Versus Percent Load.

Figures 12 and 13 reveal why measured vibration due to unbalance during test stand operation cannot be compared to rotordynamic calculations for even partial load field conditions that are provided as requirements of API 613 (1995).

Figure 14 shows the pinion extended shaft end with field coupling hub, adapter plate, and shop coupling spacer installed. The coupling half weight in the field was reported to be 362 lb compared to the shop arrangement which yielded 512 lb. Response to unbalance calculations were made for the 2 percent load shop condition (coupled case) as well as three other configurations. First the shop coupling spacer was removed and an uncoupled case calculated. Then the adapter plate was removed (hub only case) and next the hub was removed (shaft only case). In each successive case the load vector on the pinion bearings was reduced slightly and a different overhung mass existed. These effects should increase the critical speed with each successive modification to the rotordynamic model. Table 3 summarizes results for the first critical speed in horizontal and vertical directions for the various configurations. The first group of values for shop conditions with a 20 mil bearing clearance show the first critical speed could be in a range of 5100 to 8500+ rpm horizontally and from 5800 to 8500+ rpm vertically depending on the support stiffness and configuration. The split critical is due to the assumption that vertical support stiffness is greater than horizontal support

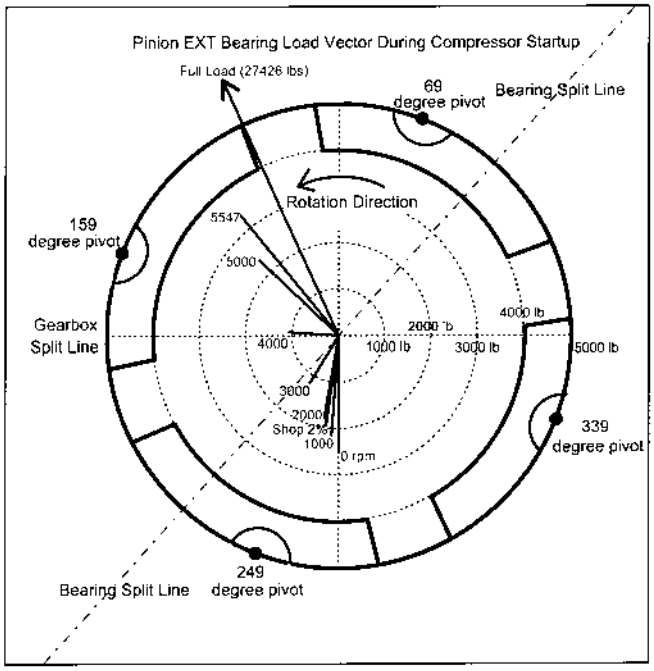

Figure 13. Bearing Load During Startup Relative to Tilting Pads.

stiffness. Thus, the vertical critical speed should be higher than the horizontal critical speed for any selected combination of support stiffness and configuration. Also, depending on the selected combination, the critical speed could be calculated to encroach upon running speed of 5547 rpm.

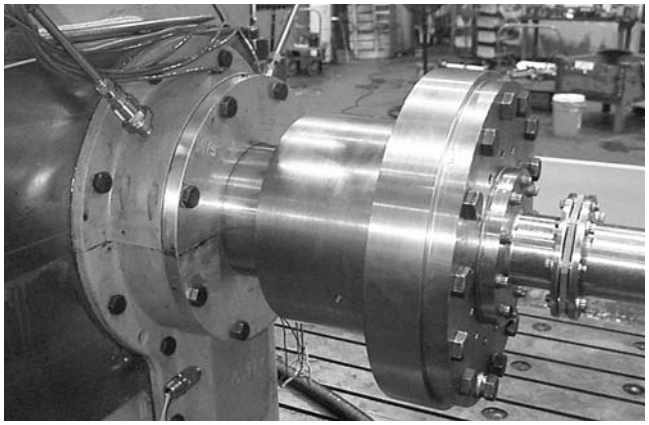

Figure 14. Pinion Extended End with Shop Coupling Installed.

MORE SHOP TESTS

Response to unbalance for all four of the above referenced configurations was measured on the test stand. Figure 15 summarizes results for the extended end bearing 1× vibration versus speed for three of these cases. Two peaks are seen in each curve on the graph. The lower peak is in the 5500 to 5600 rpm range for each case and did not show the increase in frequency as would be expected of a critical speed based on rotordynamic calculations. The upper peak in each curve did respond as expected with incremental steps in peak frequency as the coupling parts were removed. Table 4 captures the results of the tests for each peak in horizontal and vertical directions for shop conditions with a 20 mil bearing clearance. An alarming result is evident. If these peaks represent the horizontal and vertical shaft critical speeds due to oil film and support stiffnesses, then the vertical values should

Table 3. Rotordynamic Calculation Summary.

Extended End with Coupling Unbalance

Configuration	Horizontal Peak, RPM		Vertical Peak, RPM	
	Soft Supports	Hard Supports	Soft Supports	Hard Supports
Shop Conditions 20 mil clearance				
Coupled - 2 % load	5100	5820	5800	6300
Uncoupled	5440	6300	6300	6900
Hub Only	6160	8240	8080	8500+
Shaft Only	8500+	8500+	8500+	8500+
Shop Conditions 15 mil clearance				
Coupled - 2 % load	5640	6640	6520	7140
Uncoupled	6000	7170	6980	7720
Hub Only	6760	8160	8500+	8500+
Shaft Only	7340	8500+	8500+	8500+
Field Conditions 20 mil clearance				
100 % load	6600	7160	7280	7740
Field Conditions 15 mil clearance				
100 % load	6980	7540	7880	8500+
50 % load	6800	7480	7620	8180
25 % load	6720	7460	7500	8040
Startup	6720	7460	7500	8060

be higher than the horizontal values, but this was not the case. The horizontal values went from 6500 to 6900 rpm but the vertical values went from 5500 to 5600. Recalling that the data were only recorded approximately every 100 rpm indicates the vertical values are essentially constant. This fact, coupled with the inverse order between horizontal and vertical directional peaks, gave rise to the thought that the vertical direction peak may not be due to rotordynamics but could be structural in nature.

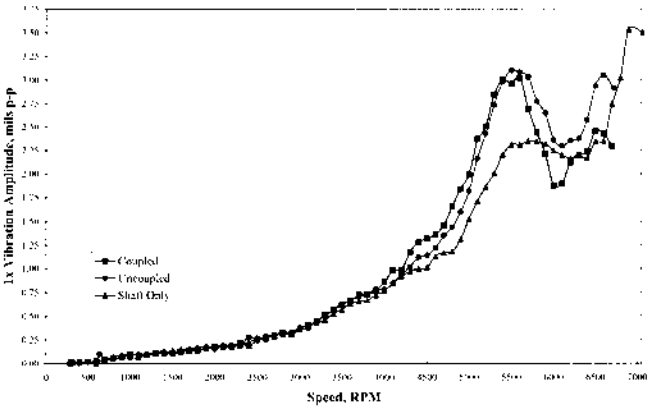

Figure 15. Measured Pinion Extended End 1× Response to Coupling Unbalance Comparison.

Table 4. Measured Vibration Summary.

Extended End with Coupling Unbalance

Configuration	Horizontal Peak RPM	Vertical Peak RPM
Shop Conditions 20 mil clearance		
Coupled - 2 % load	6500	5600
Uncoupled	6600	5500
Shaft Only	6900	5500

Other recorded vibration and static bearing operating data were discovered that further supported the conclusions reached above that both these peaks could not be from the split critical. Figure 16 illustrates the shaft centerline position as a function of speed as measured on the test stand. Normally this curve should rise from the bottom center of the bearing and move away from the mesh slightly. The measured data show the expected trend up to about 4500 rpm. Then the shaft center continues to move away from the mesh but droops with increasing speed. This indicated another controlling phenomena was influencing the bearing characteristics. Also, the measured shaft filtered 1× vibration orbit clearly showed the 5600 rpm resonance to be an almost purely vertical mode, as seen in Figure 17. The orbit shows a vertical amplitude of approximately 4 mils (peak-to-peak) and less than 1 mil horizontally. In light of these data there was no mistaking this peak as part of a split critical speed.

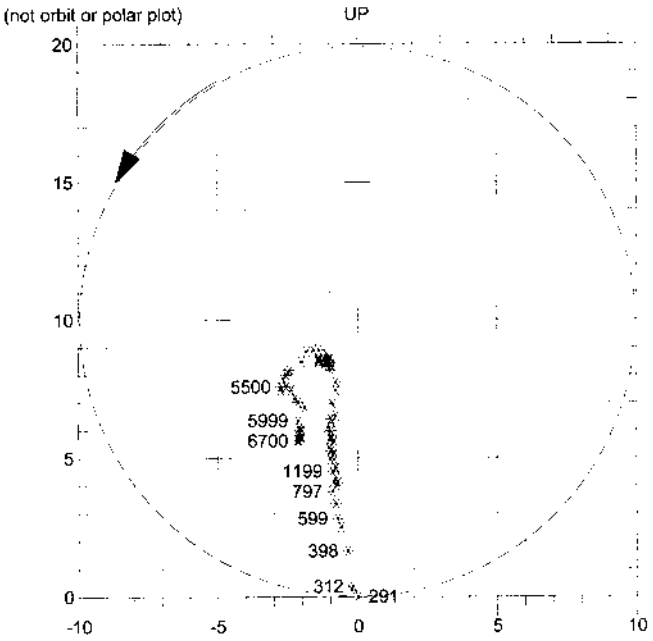

Figure 16. Measured Shaft Centerline Versus Speed Shown Relative to Bearing Clearance Circle.

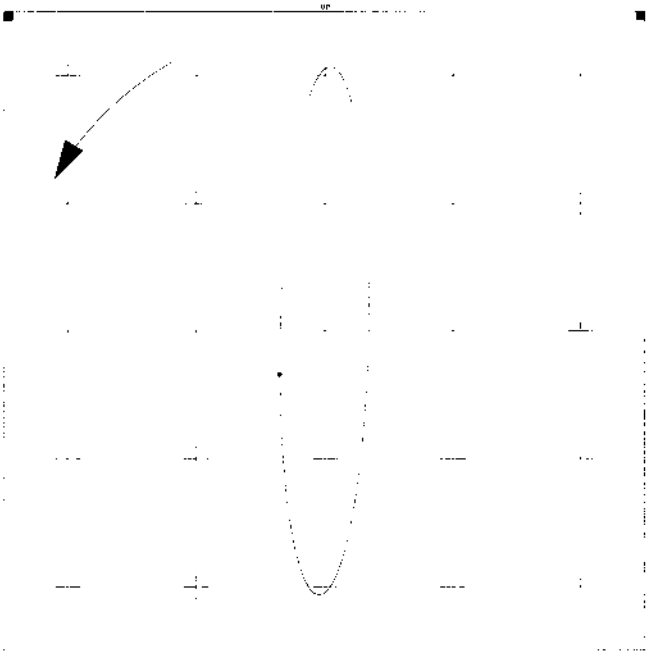

Figure 17. Orbit of 1× Vibration on Resonance at 5600 RPM.

IMPACT TESTS

Impact tests were conducted with the unit not operating. An accelerometer with a magnetic base was used to measure response from impact (hammer blows). Casing response was measured at both ends with hammer blows applied to the casing. The pinion was also bumped laterally and axially while sitting in the unit, with the accelerometer attached to the pinion. At locations where the accelerometer was attached to the casing, no significant casing resonance or lateral pinion resonance was detected at frequencies near running speed. When the shaft was impacted axially a highly responsive resonance was found near running speed that pointed toward investigation of axial structural phenomena (Figure 18).

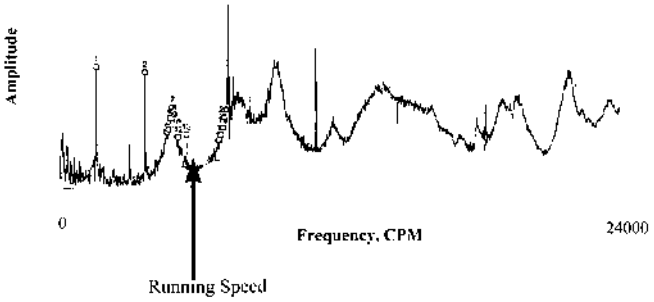

Figure 18. Impact Data on Pinion with Gear Unit Not Running.

BEARING MODIFICATIONS AND RESULTS

It was decided to modify the pinion bearings to return them to the originally designed clearance and preload to assure a higher critical speed. If under test stand conditions there were two overlapping resonances near operating speed, the measured vibration response to unbalance would be magnified by both. Returning the bearings to the original design clearance to increase to critical speed could reduce the amplification and possibly negate the need to address any structural resonance. The oil drain and end seal modifications previously installed remained and were enhanced by extending the bearing's side drain outlet angular extent. These modifications were installed and run with no other changes to the unit.

The resulting bearing pad temperatures were in the acceptable range even with the tighter clearance and the shaft critical speeds were seen to be increased. However, the additional separation of the shaft critical and the *other* resonance were not enough to prevent the resonance near running speed from being a problem. This conclusively showed the resonance near running speed was not a shaft critical but most likely a structural resonance. With this as the only likely culprit available to blame it was decided to investigate probable gear case structural modes that could exist near running speed.

FINITE ELEMENT ANALYSIS OF GEAR UNIT

Modal analysis of the gear unit was performed using the finite element method. Modeling, analysis, and review of results were done with Pro/MECHANICA® software.

A linear elastic finite element model of the gear unit was created. The model included the gear case as well as the bearings, pinion, and gear. Mass, spring, beam, and shell elements were used. The foundation was modeled with springs rigidly constrained at one end and attached to the casing at the other. The casing consisted of shell elements. Springs between the casing and rotors represented the vertical and horizontal stiffness of the radial bearings and the axial restraint of the thrust bearing on the gear shaft. Beams were used for the pinion and gear, as well as the foundation to casing transition, and casing to bearing transition. Finally, masses were used to represent some parts that were not otherwise modeled. The result was a relatively simple model. However, it contained sufficient detail to make a good approximation of shape, stiffness, and mass of individual parts and of the unit as a whole. This approach permitted rapid modeling and analysis and it produced results that agreed satisfactorily with test data.

First, analysis was done to evaluate the significance of the test stand floor stiffness. Analyses at low, medium, and high estimated support stiffnesses showed this was not likely a source of trouble nor a means of solving the problem. All subsequent analyses were made with the medium support stiffness.

Second, mode shapes and frequencies for the original casing design with *soft* bearings were evaluated, which corresponded to the 20 mil clearance at low load. The results showed two endwall *breathing* modes involving the entire gear case in the vicinity running speed. As with all finite element work, extreme care must be taken when investigating modes and comparing to measured data. Review of the results showed the two modes near running speed warranted further investigation and that the model gave a fair representation of the actual system. Based on the critical timing to diagnose and resolve the problems and get the gear unit shipped, the model was not *calibrated* further.

The two modes being investigated were referred to as modes *eight* and *nine*. Both involved endwall *breathing* of the gear case. Mode eight was below running speed and mode nine was above running speed. Table 5 summarizes the calculated frequencies for modes eight and nine for the pertinent finite element cases.

Table 5. Finite Element Analysis Summary.

Modes Eight and Nine				
Bearing	Load	Tie Bar	Mode Eight CPM	Mode Nine CPM
Soft	Shop	No	4996	5803
Stiffer	Shop	No	5056	6096
Stiffer	Shop	Yes	5342	6660
Stiffest	Field	Yes	5786	7080

Figure 19 illustrates the alternating maximum deflections of mode shape nine as viewed across the gear unit from the pinion side. The extended (coupling) end of the pinion is on the left in the figure. The upper view in the figure is for the gear unit pitching left while the bottom view is for the gear unit pitching right. This case motion caused significant pinion motion vertically with opposite ends of the shaft out of phase but caused little horizontal pinion motion. This mode best matched the measured test stand orbit data. The mode could be easily excited by unbalance at the coupling and aggravated by its overhung moment. The portions of the gear case endwalls above each pinion bearing were out of phase with each other and the distortion of one endwall was much greater than the other. An unbalance force applied at the coupling could drive this structural mode causing a resonant condition. The resulting motion in turn could cause radial displacement of the pinion thus increasing the eccentricity of any unbalanced mass at the coupling, which would further increase the unbalance force. Obviously, mechanical restraints limit the total motion of the system, which could be thought of as a parametric excitation phenomenon.

The finite element model was then used to evaluate possible design modifications aimed at raising the frequency of the mode near running speed. Bearing changes described above to return the clearance and preload to original design values were evaluated first. The model was updated to reflect the pinion bearing stiffness

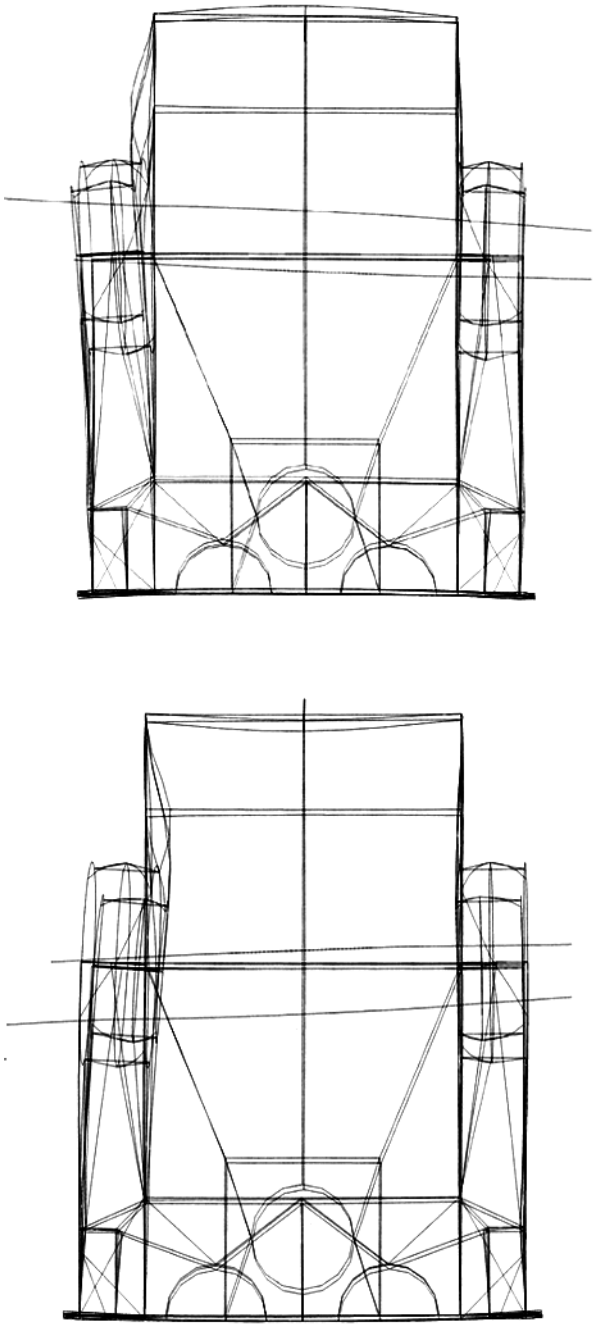

Figure 19. Gearcase Mode Shape Near Operating Speed Predicted by Finite Element Analysis.

increase of roughly a factor of two. However, the stiffness was still relatively low since shop testing was being done with only a light load on the gearbox. The modal analysis was repeated with the change. Results listed in Table 5 show this had a small effect on the calculated frequency of the modes of primary interest near running speed. This correlated with the measured results with the stiffer bearings.

The next step was to consider structural changes suggested by examination of the mode shapes found in preceding analyses. The most feasible possibility was to install a tie between the endwalls of the casing in hopes of raising the frequencies of the breathing modes. Therefore, a tie was added to the model for the next analysis run. Results showed a significant increase in frequency for mode nine. Finally, pinion bearing stiffness was roughly doubled again to represent conditions that might be seen in actual operation under full load in the field. The combined effects of increased bearing stiffness and the gear case structural change appeared sufficient to ensure that the mode nine resonance would no longer be of concern.

Table 5 shows an increase in frequency for mode eight due to the tie bar and bearing modifications from below running speed to just above running speed. Mode shape evaluation and comparison to measured test results gave confidence that this mode was not causing the problems identified by the measured vibrations.

TIE BAR INSTALLATION

Based on the analyses described above, it was decided to install a tie bar axially across the gear case upper section. The tie bar assembly connected the gear case walls just above the gear mesh and bearings. It extended across the axial length of the inside of the gear case cover and was parallel to the pinion. It included a heavy wall steel tube between the casing walls with a steel rod inside the tube as shown in Figure 20. The tube was accurately fitted between machined pads in the casing to avoid distorting the casing when the assembly was tightened. Threaded portions of the rod protruded through the walls, with a nut at one end and a stud tensioner at the other. The tensioner had multiple jackbolts that held the entire assembly tight. O-ring seals at the ends of the tube prevented leakage of oil. Figure 21 shows a view inside the gear case cover with the tie bar installed. The gear mesh cooling oil spray nozzles can be seen near the tie bar, which blocks a portion of the spray. Figure 22 is an overall view of the gear unit on the test stand. The tie bar end can be seen just above the pinion bearing housing. Figure 23 is a closeup view of the stud tensioner being installed.

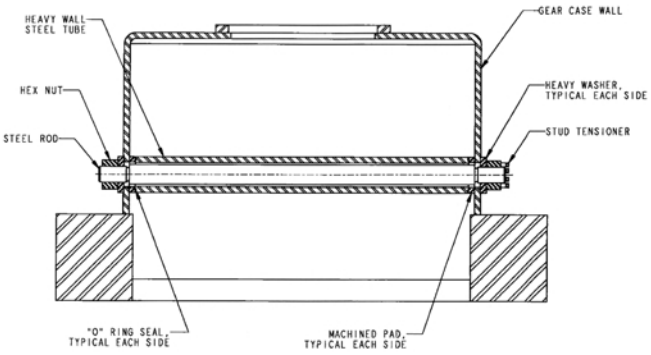

Figure 20. Section Through Gearcase Cover Showing Tie Bar Details.

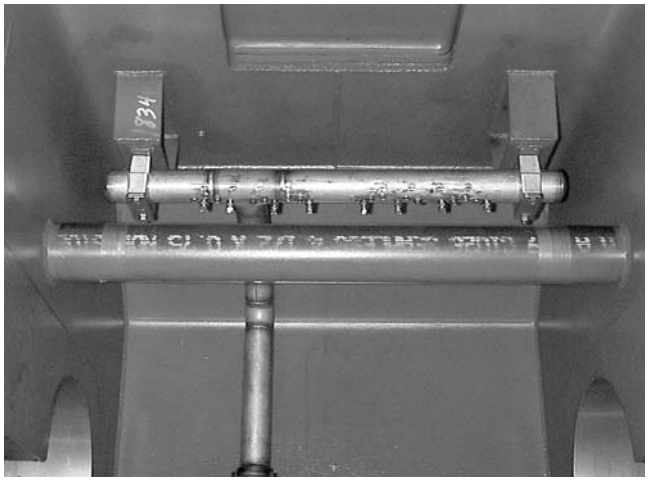

Figure 21. View of Inside of Gearcase Cover Showing Tie Bar Installed.

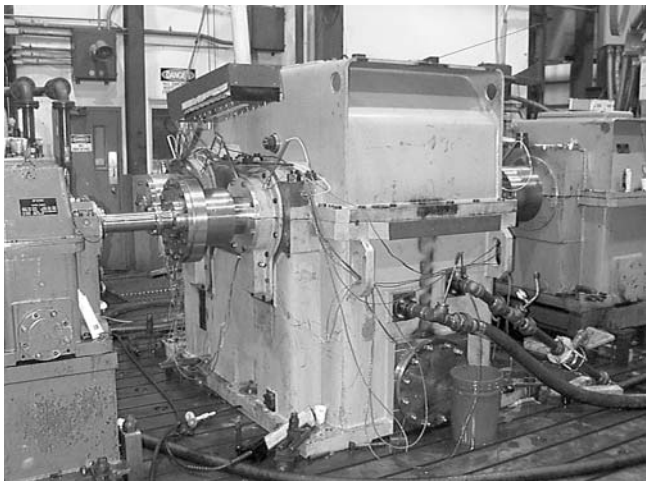

Figure 22. Gear Unit on Test Stand with Tie Bar Installed.

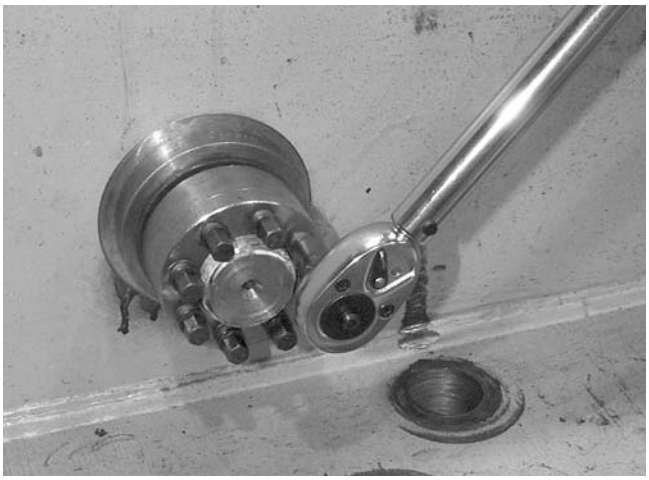

Figure 23. End of Tie Bar with Positive Tensioning Device.

Should the analysis results and decision to ignore mode eight be found to be in error, the tie bar could be easily removed and/or modified.

FINAL TEST AND RESOLUTION

With the tie bar and the previously described and tested bearing modifications installed, the unit was assembled for test stand operation and tested as before. First a run was made with the shop coupling installed with a 2 percent load. Then the coupling was removed a piece at a time and runs were made to compare directly to previous data. Figure 24 shows a comparison of the uncoupled case before and after the modifications. The resonance previously near running speed was found to be much higher in frequency near 6600 to 6700 rpm, which was outside the 20 percent separation margin required. Bearing temperatures were within the specified limits. Mode eight was not seen in the measured data. Based upon successful completion of the tests the unit was accepted and shipped.

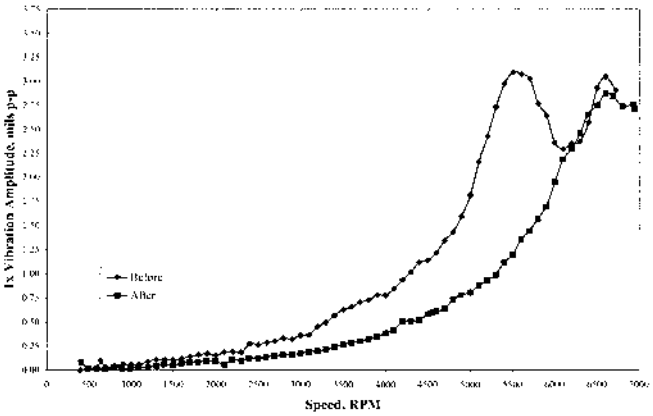

Figure 24. Comparison of 1× Vibration Before and After Tie Bar Installation.

CONCLUSION

Two resonant phenomena occurred to aggravate pinion running speed vibrations during test stand acceptance runs. One was a shaft critical and the other was a structural mode. Both were being excited by coupling unbalance. Two resonances within close proximity of each other resulted in unacceptable pinion vibration. Bearing modifications fixed the critical speed problem while a structural modification fixed the other. Tests with all modifications installed proved the gear unit met the specified purchase requirements.

REFERENCES

API Standard 613, 1995, "Special Purpose Gear Units for Petroleum, Chemical, and Gas Industry Services," Fourth Edition, American Petroleum Institute, Washington, D.C.

Nicholas, J. C., Rotating Machinery Technology, Inc., 1998, "Pad Bearing Assembly with Fluid Spray and Blocker Bar," United States Patent No. 5,738,447.

Pro/MECHANICA®, Parametric Technology Corporation (PTC), Waltham, Massachusetts.